論文 5-2-5

간단한 시간 지연 관측기를 이용한 영구자석 동기전동기 구동 강인 전류제어 기법

金 庚 和, 尹 明 重

A Robust Current Control Technique with a Simple Time Delayed Estimator for a Permanent Magnet Synchronous Motor Drive

Kyeong-Hwa Kim, Myung-Joong Youn

요 약

간단한 시간 지연 관측기를 이용한 영구자석 동기전동기의 강인 전류 제어 기법이 제시된다. 전압원 인버터 구동 영구자석 동기전동기의 전류 제어 기법 중 예측형 전류 제어가 우수한 성능을 주는 것으로 알려져 있지만 이 기법은 전동기 파라미터와 동작 조건에 대한 모든 정보를 필요로 하며 전동기와 제어기의 파라미터가 일치하지 않을 경우 응답 성능이 저하되게 된다. 이러한 제한 점을 극복하기 위해 시간 지연 제어 기법을 사용하여 파라미터 변화에 의한 외란 성분이 추정되고 이는 전향 제어 방식으로 기준 전압의 계산에 이용된다. 이를 통해 제어기 성능이 매우 간단한 방식으로도 상당히 향상됨을 입증한다. 제안된 제어 방식의 타당성이 비교 시뮬레이션과 실험을 통해 입증된다.

ABSTRACT

A robust current control technique with a simple time delayed estimator for a permanent magnet synchronous motor (PMSM) drive is presented. Among the various current control schemes for a voltage source inverter-fed PMSM drive, the predictive control is known to give a superior performance. This control technique, however, requires the full knowledge of machine parameters and operating conditions, and gives an unsatisfactory response under the parameter mismatch between the motor and controller. To overcome such a limitation, the disturbances caused by the parameter variations will be estimated by using a time delay control approach and used for the computation of the reference voltages by a simple feedforward control. The proposed control scheme is implemented on a PMSM using the software of DSP TMS320C30 and the effectiveness is verified through the comparative simulations and experiments.

Key Words : Robust current control, Time delayed estimator, PMSM, Inverter, DSP

1. Introduction

The current control schemes for a voltage source inverter-fed PMSM drive can be classified as the hysteresis control, ramp comparison control, synchronous frame proportional integral (PI) control, and predictive control.[1-11] The basic requirements for the current controller are the fast dynamic response during the transient state, lower current ripple in the steady-state, stable PWM inverter operation, and robustness against the variations of machine parameters. The hysteresis current control has the advantages such as a fast transient response and a simple implementation. However,

because of large current errors and an irregular PWM inverter operation, this scheme cannot be used in a high performance drive system.[4] The ramp comparison current control scheme gives a constant switching frequency. However, there are some unavoidable limitations such as a steady-state error and a phase delay in the steady-state since this controller is designed in the stationary reference frame where P or PI controller can not exactly track the sinusoidally varying reference.[4] To overcome such a limitation, a synchronous frame PI current regulator has been proposed.[5] In the synchronous frame PI current regulator, the regulated currents are dc quantities rather than the variables as in the stationary reference frame. By employing the PI control and cancellation inputs for the back EMF and cross-coupling terms, this control gives an ideal steady-state control characteristics irrespective of operating conditions. However, the transient response is generally slow or may be degraded due to the inexact cancellation input under the parameter variations. On the other hand, in a predictive control scheme, the switching instants of the inverter switches are determined by calculating the required voltage which forces the motor currents to follow their references. With the space vector PWM technique, this control scheme is known to provide the advantages such as a constant switching frequency and a lower current ripple.[6,7] This scheme, however, requires the full knowledge of machine parameters and operating conditions with the sufficient accuracy, and gives an unsatisfactory response under the parameter mismatch between the motor and controller. Generally, it is very difficult to exactly obtain the informations on the machine parameters since they may vary during operation due to the changes in the temperature, current level, and operating frequency. In particular, the inaccuracy of the back EMF influences primarily on the control performance. To overcome such a problem, a current control scheme independent of the back EMF variation has been proposed.[8] The basic assumption is that the back EMF is constant between each sampling instant. Based on this, the back EMF has been estimated by using the feedback of the delayed input voltages and currents in a discrete domain. Thus, a robust control performance against the back EMF variation can be obtained. This scheme still, however, requires other motor parameters such as the stator resistance and stator inductance, and furthermore, the experimental verification has not been proved. Recently, a multivariable state feedback control with an integrator[9] and a generalized predictive control[10] have been reported. Although a good performance can be obtained, the controller design is quite complex.

In recent years, time delay control schemes have been suggested as an effective way for a control of systems with unknown dynamics and uncertainties since these schemes require little a priori knowledge of the dynamics of the system [12-13]. The basic idea is to approximate a disturbance or uncertainty with the time-delayed value of control inputs and derivatives of state variables at the previous time step. This algorithm does not require an explicit dynamic model nor does it depend on the estimation of specific parameters. Instead, it uses informations in the past to directly estimate the unknown dynamics or uncertainties at any given instant through the time delay [12].

This paper presents a robust current control technique with a simple time delayed estimator for a PMSM drive. Although the predictive control provides an ideal response and a stable performance independent of the operating condition, its steady-state response may be degraded under the motor parameter variations such as the flux linkage, stator inductance, and stator resistance. This is more serious at high speed operations since the disturbance is proportional to the product of the operating speed and these parameters. To overcome this drawback, the disturbance caused by the parameter variations will be estimated by using a time delay control approach and used for the calculation of the reference voltages by a feedforward control. Thus, the steady-state control performance can be significantly improved, while

retaining the good characteristics of the predictive control. Since the disturbance compensation can be accomplished in an extremely simple manner, an improved robustness against the parameter variations can be obtained without requiring a much more complex controller design such as the methods in [8-10]. The whole control system is implemented by the software of DSP TMS320C30 for a PMSM driven by a three-phase voltage fed PWM inverter.

2. Modeling of PMSM

The stator voltage equations of a PMSM in the synchronously rotating reference frame are described as follows [11]:

$$v_{qs} = R_s i_{qs} + L_s \dot{i}_{qs} + L_s \omega_r i_{ds} + \lambda_m \omega_r \tag{1}$$

$$v_{ds} = R_s i_{ds} + L_s \dot{i}_{ds} - L_s \omega_r i_{qs} \tag{2}$$

where R_s is the stator resistance, L_s is the stator inductance, ω_r is the electrical rotor angular velocity, and λ_m is the flux linkage established by the permanent magnet. From (1) and (2), the discrete-time equation can be obtained as follows:

$$v_{qs}(k) = R_s i_{qs}(k) + \frac{L_s}{T}[i_{qs}(k+1) - i_{qs}(k)] + L_s \omega_r i_{ds}(k) + \lambda_m \omega_r \tag{3}$$

$$v_{ds}(k) = R_s i_{ds}(k) + \frac{L_s}{T}[i_{ds}(k+1) - i_{ds}(k)] - L_s \omega_r i_{qs}(k) \tag{4}$$

where T is a sampling period. Using the nominal parameters, (3) and (4) can be rewritten as follows:

$$v_{qs}(k) = R_{so} i_{qs}(k) + \frac{L_{so}}{T}[i_{qs}(k+1) - i_{qs}(k)] + L_{so} \omega_r i_{ds}(k) + \lambda_{mo} \omega_r + f_q(k) \tag{5}$$

$$v_{ds}(k) = R_{so} i_{ds}(k) + \frac{L_{so}}{T}[i_{ds}(k+1) - i_{ds}(k)] - L_s \omega_r i_{qs}(k) + f_d(k) \tag{6}$$

where $f_q(k)$ and $f_d(k)$ represent the disturbances caused by the parameter variations. These can be expressed as

$$f_q(k) = \Delta R_s i_{qs}(k) + \frac{\Delta L_s}{T}[i_{qs}(k+1) - i_{qs}(k)] + \Delta L_s \omega_r i_{ds}(k) + \Delta \lambda_m \omega_r \tag{7}$$

$$f_d(k) = \Delta R_s i_{ds}(k) + \frac{\Delta L_s}{T}[i_{ds}(k+1) - i_{ds}(k)] - \Delta L_s \omega_r i_{qs}(k) \tag{8}$$

where $\Delta R_s = R_s - R_{so}$, $\Delta L_s = L_s - L_{so}$, $\Delta \lambda_m = \lambda_m - \lambda_{mo}$ and subscript "o" denotes the nominal value.

3. Disturbance Estimation Using Time Delay Control Approach

In the time delay control, in order to obtain the estimates for the disturbances $f_q(t)$ and $f_d(t)$ in the continuous-time domain, it is considered that the values of $f_q(t)$ and $f_d(t)$ at the present time t are very close to those at time $t-\tau$ in the past for a small time delay τ as follows [12,13]:

$$f_q(t) = f_q(t-\tau) \tag{9}$$

$$f_d(t) = f_d(t-\tau) \tag{10}$$

In the discrete-time domain, (9) and (10) can be expressed as follows:

$$f_q(k) \cong f_q(k-L) \tag{11}$$

$$f_d(k) \cong f_d(k-L) \tag{12}$$

where $\tau = LT$ and L is a positive integer. By approximating the disturbances at the present time k with those of (k-L)-th time step and using (5) and (6), the simple estimates for the disturbances can be derived as follows:

$$\hat{f}_q(k) \cong f_q(k-L) = v_{qs}(k-L) - R_{so} i_{qs}(k-L) - \frac{L_{so}}{T}[i_{qs}(k-L+1) - i_{qs}(k-L)] - L_{so} \omega_r i_{ds}(k-L) - \lambda_{mo} \omega_r \tag{13}$$

$$\hat{f}_d(k) \cong f_d(k-L) = v_{ds}(k-L) - R_{so} i_{ds}(k-L) - \frac{L_{so}}{T}[i_{ds}(k-L+1) - i_{ds}(k-L)] + L_{so} \omega_r i_{qs}(k-L) \tag{14}$$

where the symbol "^" denotes the estimated quantities. Although the unknown disturbances can be simply estimated, this technique has some limitation. Since the numerical differentiation of the measured current is needed for the estimation of disturbances $\hat{f}_q(k)$ and $\hat{f}_d(k)$, the high frequency

noise in stator currents may be amplified. A low pass filter is employed to reduce this noise. This is done in a digital manner within DSP. A simple first order low pass filter can be expressed in the continuous-time domain as follows:

$$G(s)=\frac{a}{s+a} \tag{15}$$

where a denotes the cut-off frequency of the filter. For the digital implementation, (15) is discretized using the bilinear transform method where the Laplace operator s is replaced as follows[14]:

$$s=\frac{2}{T}\frac{1-z^{-1}}{1+z^{-1}} \tag{16}$$

By substituting (16) into (15), the discrete-time transfer function can be obtained as follows:

$$G(z)=\frac{\hat{f}_{qf}(z)}{\hat{f}_{q}(z)}=\frac{aT(1+z^{-1})}{(2+aT)-(2-aT)z^{-1}} \tag{17}$$

Using (17), the filtered estimate for the q-axis disturbance can be obtained in a difference equation as follows:

$$\hat{f}_{qf}(k)=\frac{2-aT}{2+aT}\hat{f}_{qf}(k-1)+\frac{aT}{2+aT}[\hat{f}_{q}(k)+\hat{f}_{q}(k-1)] \tag{18}$$

Similarly, the filtered estimate for the d-axis disturbance can be obtained as follows:

$$\hat{f}_{df}(k)=\frac{2-aT}{2+aT}\hat{f}_{df}(k-1)+\frac{aT}{2+aT}[\hat{f}_{d}(k)+\hat{f}_{d}(k-1)] \tag{19}$$

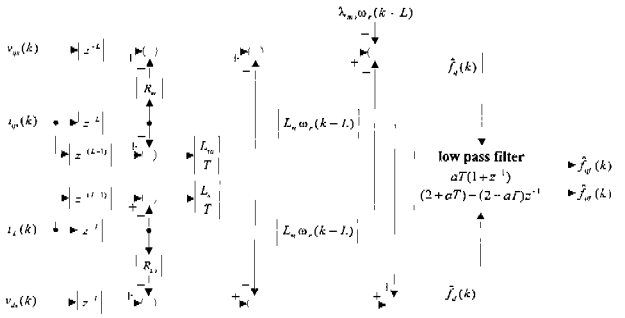

Fig. 1 Disturbance estimation using time delay control

Fig. 1 shows the proposed disturbance estimation scheme using the time delay control. The measured currents and voltages are delayed by L step and these delayed signals are used for the estimation of disturbances. Since this can be accomplished by only using the time delay of L step, some calculations, and low pass filter, the computational load for the controller is negligibly small.

4. Current Control with Feedforward Didturbance Compensation

The steady-state control performance of the predictive current control can be significantly improved through the use of a disturbance compensation technique, while retaining its good dynamic performance. By employing the estimated disturbances $\hat{f}_q(k)$ and $\hat{f}_d(k)$ for a feedforward control and using the conventional predictive control, the reference voltages in the proposed control scheme are calculated as follows:

$$v_{qs}^{*}(k)=R_{so}i_{qs}(k)+\frac{L_{so}}{T}[i_{qs}^{*}(k+1)-i_{qs}(k)]+L_{so}\omega_r(k)i_{ds}(k)+\lambda_{mo}\omega_r(k)+\hat{f}_{qf}(k) \tag{20}$$

$$v_{ds}^{*}(k)=R_{so}i_{ds}(k)+\frac{L_{so}}{T}[i_{ds}^{*}(k+1)-i_{ds}(k)]-L_{so}\omega_r(k)i_{qs}(k)+\hat{f}_{df}(k) \tag{21}$$

where the symbol "*" denotes the reference quantities. Then, the reference voltages are composed of the conventional predictive control part and disturbance compensation part.

The steady-state performance due to the inaccuracy of the machine parameters can be obtained from the reference voltages and the discrete-time voltage equations in (5) and (6). In the case of the predictive control without a feedforward compensation, the q-axis and d-axis current errors at the (k+1)-th sampling instant can be derived from the reference voltages and the discrete-time voltage equations as follows:

$$i_{qs}^{*}(k+1)-i_{qs}(k+1)=\frac{T}{L_{so}}f_q(k) \tag{22}$$

$$i_{ds}^{*}(k+1)-i_{ds}(k+1)=\frac{T}{L_{so}}f_d(k) \tag{23}$$

Clearly, the steady-state errors are proportional to the magnitude of disturbances which is the function of an operating speed and a load condition. The

steady-state q-axis and d-axis current errors of the predictive control at the (k+1)-th sampling instant due to the inaccuracy of the individual machine parameters are summarized in Table 1. On the other hand, the steady-state errors of the proposed control scheme at the (k+1)-th sampling instant can be obtained as follows:

$$i_{qs}^{*}(k+1)-i_{qs}(k+1)=\frac{T}{L_{so}}e_q(k) \tag{24}$$

$$i_{ds}^{*}(k+1)-i_{ds}(k+1)=\frac{T}{L_{so}}e_d(k) \tag{25}$$

where

$e_q(k)=f_q(k)-\hat{f}_{qf}(k), \qquad e_d(k)=f_d(k)-\hat{f}_{df}(k).$

Unlike the conventional predictive control, the current errors of the proposed scheme are proportiov -nal to the estimation error of the disturbances.

Table 1 Steady-state current errors of predictive control due to the inaccuracy of individual machine parameters

	$i_{qs}^{*}(k+1)-i_{qs}(k+1)$	$i_{ds}^{*}(k+1)-i_{ds}(k+1)$
ΔR_s	$\Delta R_s(T/L_{so})i_{qs}(k)$	$\Delta R_s(T/L_{so})i_{ds}(k)$
ΔL_s	$(\Delta L_s/L_{so})[i_{qs}(k+1)-i_{qs}(k)]$ $+\Delta L_s(T/L_{so})\omega_r(k)i_{ds}(k)$	$(\Delta L_s/L_{so})[i_{ds}(k+1)-i_{ds}(k)]$ $-\Delta L_s(T/L_{so})\omega_r(k)i_{qs}(k)$
$\Delta\lambda_m$	$\Delta\lambda_m(T/L_{so})\omega_r(k)$	0

5. Configurations of the Overall System

The overall block diagram for the proposed control scheme is shown in Fig. 2. The overall system consists of a proposed current controller, a time delayed disturbance estimator, a PWM inverter, and a PMSM. For the current control algorithm, the predictive control with a simple feedforward disturbance compensation is used. During the operations, the disturbances caused by the parameter variations are estimated by using the time delay control approach. The computed reference voltages are applied to a PMSM using the space vector PWM technique [15]. Based on this, the feedback voltage for the disturbance estimation can be easily obtained from the switching states of the inverter and dc link voltage by considering the dead time of the switch.

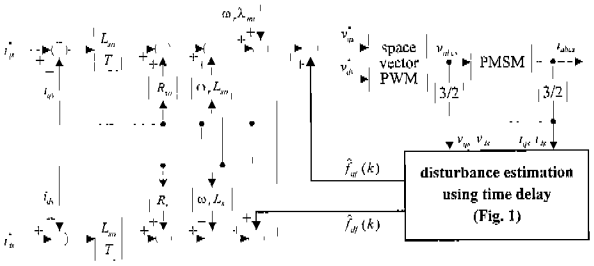

Fig. 2 Overall block diagram for the proposed current control scheme

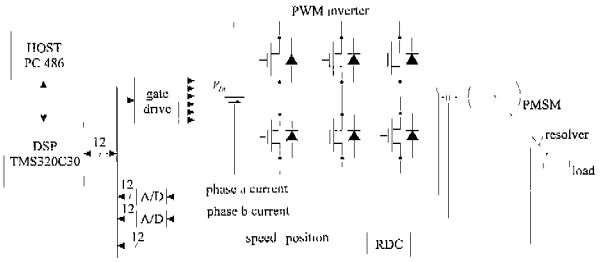

Fig. 3 Configuration of experimental system

The configuration of the experimental system is shown in Fig. 3. The whole control algorithms are implemented by the assembly language program using DSP TMS320C30 [16]. The sampling period is set to 128 [sec], which yields a switching frequency of 7.8 kHz. The PMSM is driven by a three-phase PWM inverter employing the intelligent power module (IPM). The nominal parameters of a PMSM are listed in Table 2.

Table 2 Specifications of a PMSM

Rated power	400 W	Rated speed	3000 rpm
Rated torque	1.274 Nm	Number of poles	4
Magnetic flux	0.16 Wb	Stator resistance	3.0 Ω
Stator inductance	5 mH	Moment of inertia	1.54×10^{-4} Nm s^2

5. Simulations and Experimental Results

Fig. 4 shows the simulation results for the proposed scheme at steady-state under the parameter variations ($\Delta\lambda_m=-0.5\lambda_{mo}$, $\Delta L_s=1.0L_{so}$ and $\Delta R_s=1.0R_{so}$). The q-axis and d-axis current references are given as 2 [A] and zero, respectively, and the motor is operated at a constant speed of 1200 [rpm]. Fig. 4(a) shows the q-axis and d-axis

current responses. Fig. 4(b) shows the a-phase current at each sampling instant. Even though the predictive control gives an ideal characteristics for the nominal parameter values, the steady-state errors are observed in the q-axis and d-axis current responses under the parameter mismatch. Also, it can be shown that a phase delay exists in the phase current response. This degradation is expected to be more severe at high speed operations because the magnitude of the disturbances is proportional to an operating speed. However, as soon as the estimation algorithm starts at 25 [msec] and the estimated disturbances are used for a feedforward control, the steady-state current errors and phase delay are quickly removed within 3 [msec]. This can be explained by the estimation of the disturbance voltages as shown in Fig. 4(c). For the design of the time-delayed disturbance estimator, L=1 is chosen. Also for the cut-off frequency of the low pass filter, a=2000 is selected, which corresponds to the cut-off frequency of 318 Hz. Since the maximum electrical frequency of the PMSM is 100 Hz and the inverter switching frequency of 7.8 kHz is used, the high frequency noise caused by inverter switching can be well suppressed without affecting any influences on the fundamental current component. The corresponding a-phase current response and the current trajectory in the complex plane are shown in Fig. 4(d) and Fig. 4(e), respectively.

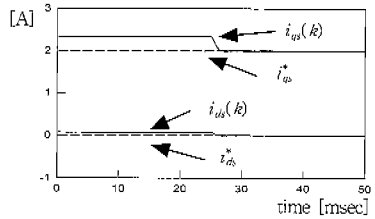

(a) q-axis and d-axis current responses

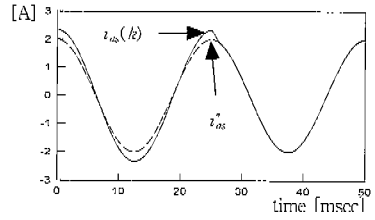

(b) a-phase current at sampling instant

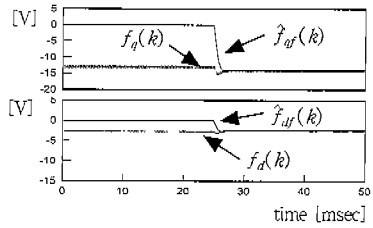

(c) estimated distsurbances

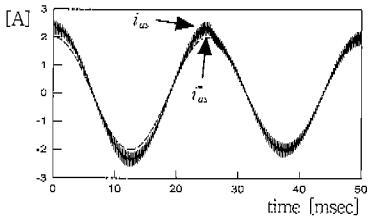

(d) a-phase current response

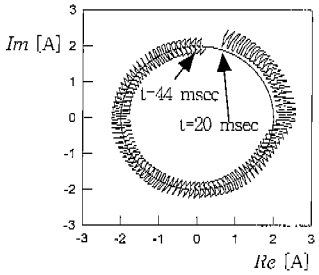

(e) current trajectory

Fig. 4 Control performance of the proposed control scheme at steady-state under the parameter variations

Fig. 5 shows the comparison of the transient response for the a-phase current. For the performance comparison with the proposed control scheme, the PI control scheme with the back EMF and cross-coupling compensation is used. The bandwidth of the PI control is selected as 4500 [rad/sec], and the same parameter variations as Fig. 4 are assumed. As can be shown in this figure, the proposed control scheme gives a faster transient response and smaller overshoot than PI control under the parameter variation.

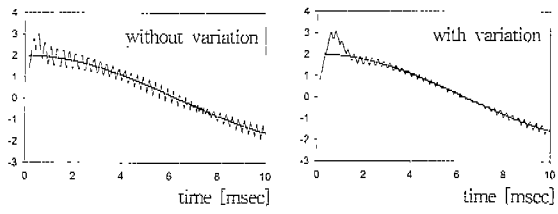

(a) PI control with the back EMF and cross-coupling compensation

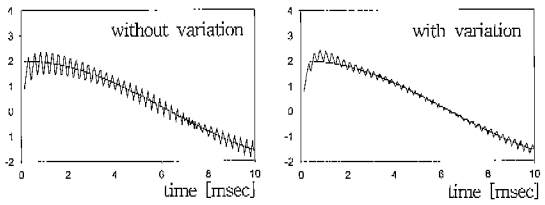

(b) proposed control scheme

Fig. 5 Comparison of transient response for a-phase current

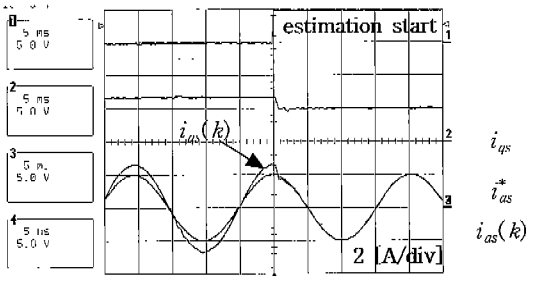

(a) q-axis current and a-phase current at sampling instant

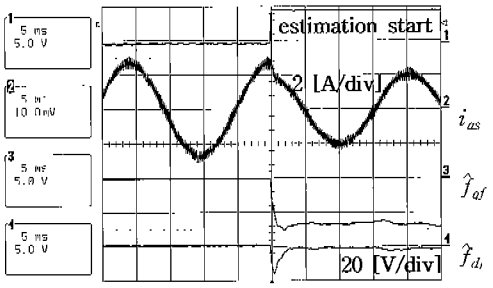

(b) a-phase current and estimated disturbances

Fig. 6 Control performance of the proposed current control scheme at steady-state under $\Delta\lambda_m$=-0.5 λ_{mo}

Fig. 6 shows the experimental results for the proposed current control scheme under $\Delta\lambda_m$=-0.5 λ_{mo}. Similarly, the q-axis and d-axis current references are given as 2 [A] and zero, respectively. Also, the experiments are carried out as the same as the simulation conditions. Before the estimation algorithm starts, a steady-state error of 0.6 [A] is observed in the q-axis current response. However, this steady-state error is removed within 3 [msec] as soon as the estimation algorithm starts. The corresponding a-phase current and the estimated disturbances are shown in Fig. 6(b).

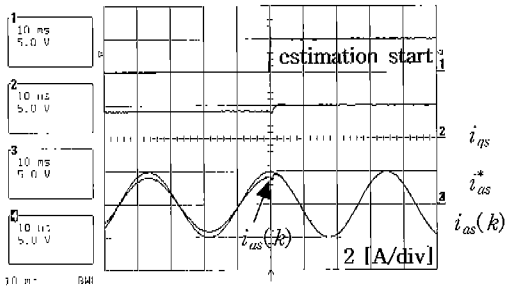

(a) q-axis current and a-phase current at sampling instant

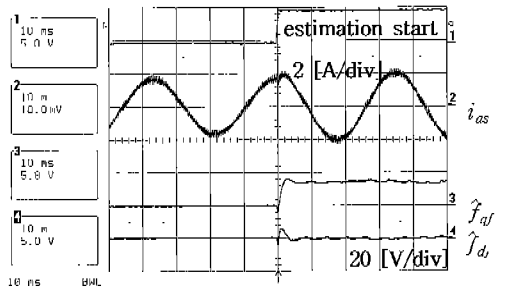

(b) a-phase current and estimated disturbances

Fig. 7 Control performance of the proposed current control scheme at steady-state under $\Delta\lambda_m$=0.5 λ_{mo}

Fig. 7 shows the control performance of the proposed scheme under $\Delta\lambda_m$=0.5 λ_{mo}. Unlike Fig. 6, since the magnitude of the flux linkage is larger in a real motor than that in a controller, the q-axis current is smaller than its reference ($i_{qs}(k)$ =1.6 [A]). However, even under this circumstance, the current is well regulated to its reference as the estimation algorithm starts. The corresponding a-phase current and estimating performance are shown in Fig. 7(b).

Fig. 8 shows the control performance of the proposed control scheme under ΔL_s=0.8 L_{so} . Before the estimation algorithm starts, the phase delay between the reference and measured value is clearly present as can be seen in Fig. 8(a). Also as can be shown in Fig. 8(b), some d-axis current exists (0.5 [A]), which degrades the performance of the maximum torque operation. However, as the estimation algorithm starts, the d-axis current is well regulated to zero and the phase delay is effectively removed even under such a large variation of L_s.

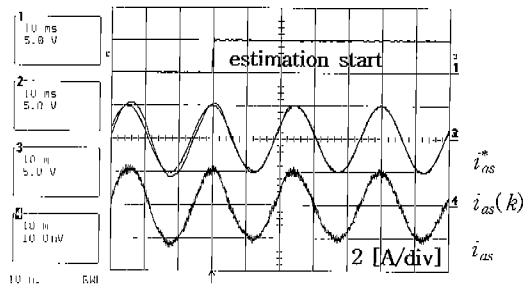

(a) a-phase current responses

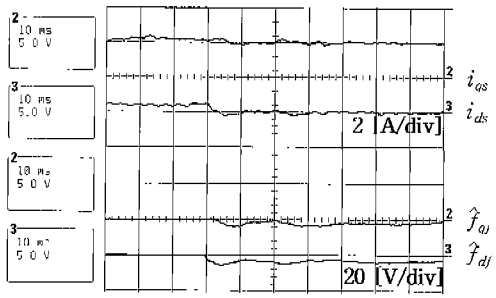

(b) q-axis and d-axis currents and estimated disturbances

Fig. 8 Control performance of the proposed current control scheme under ΔL_s=0.8 L_{so}

Figs. 9 and 10 show the current responses at starting under $\Delta\lambda_m$=-0.5 λ_{mo}.. In the conventional predictive control, the q-axis current error becomes larger since the magnitude of the disturbances is increased as the rotor speed is increased. However, by the effective disturbance estimation, the q-axis current is well controlled to its reference in the proposed scheme.

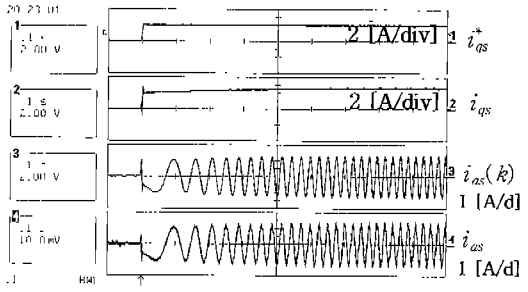

Fig. 9 Conventional predictive current control at starting under $\Delta\lambda_m$=-0.5 λ_{mo}

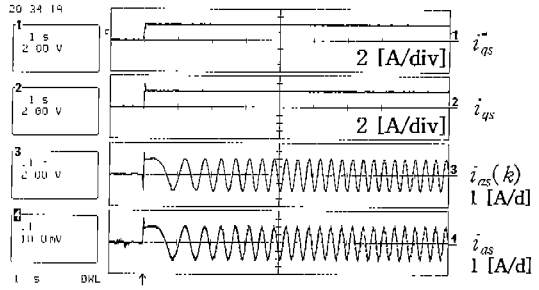

(a) current responses

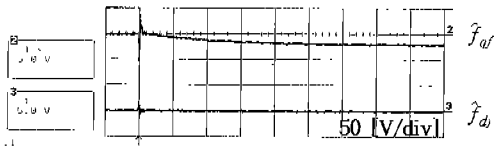

(b) estimated disturbances

Fig. 10 Proposed current control scheme at starting under $\Delta\lambda_m$=-0.5 λ_{mo}

6. Conclusions

A robust current control technique with a simple time delayed estimator for a PMSM drive is presented. Although the predictive control provides an ideal response and a stable performance, its steady-state response may be degraded under the motor parameter variations or inexact motor modeling. This is more serious at high speed regions. Even though this problem may be dealt with the conventional approaches, they require a quite complex controller design. To overcome this limitation, the disturbances caused by the parameter variations are estimated by using a time delay control approach and the estimated disturbances are used for a feedforward control. The design procedures are straightforward and the current control performance is not affected by the variations of the motor parameters and operating conditions. The whole control system is implemented using the software of DSP TMS320C30 for a PMSM driven by a three-phase voltage-fed PWM inverter and the effectiveness is verified through the comparative simulations and experiments. As a result, the current control performance can be significantly improved in an extremely simple manner.

References

[1] P. C. Krause, Analysis of Electric Machinery, New York, McGraw-Hill, 1986.

[2] T. H Liu, C. M. Young, and C. H Liu, "Microprocessor -based controller design and simulation for a permanent magnet synchronous motor drive" IEEE Trans. Ind. Elect., Vol. 35, No. 4, pp. 516-523, 1988.

[3] D. W. Novotny and R. D. Lorenz, Introduction to field orientation and high performance AC drives, IEEE IAS Tutorial Course, 1986.

[4] D. M. Brod and D. W. Novotny, "Current control of VSI-PWM inverters" IEEE Trans. Ind. Appl., Vol. 21, No. 3, pp. 562-570, 1985, May/June

[5] T.M.Rowan and R. J. Kerkman, "A new synchronous current regulator and an analysis of current-regulated PWM inverters" IEEE Trans. Ind. Appl., Vol. 22, No. 4, pp. 678-690, 1986, July/Aug.

[6] H. L. Huy and L. A. Dessaint, "An adaptive current control scheme for PWM synchronous motor drives: analysis and simulation" IEEE Trans. Power Electron., Vol. 4, No. 4, pp. 486-495, 1989, Oct.

[7] L. Ben-Brahim and A. Kawamura, "Digital control of induction motor current with deadbeat response using predictive state observer" IEEE Trans. Power Electron., Vol. 7, No. 3, pp. 551-559, 1992, July

[8] D. S. Oh, K. Y. Cho, and M. J. Youn, "A discretized current control technique with delayed input voltage feedback for a voltage-fed PWM inverter" IEEE Trans. Power Electron., Vol. 7, No. 2, pp. 364-373, 1992, April

[9] D.C.Lee, S.K.Sul, and M.H.Park, "High performance current regulator for a field-oriented controlled induction motor drive" IEEE Trans. Ind. Appl., Vol. 30, No. 5, pp. 1247-1257, 1994, Sep./Oct.

[10] L. Zhang, R. Norman, and W. Shepherd, "Long-range predictive control of current regulated PWM for induction motor drives using the synchronous reference frame" IEEE Trans. Contr. Syst. Tech., Vol. 5, No. 1, pp. 119-126, 1997, Jan.

[11] K. H. Kim, I. C. Baik, and M. J. Youn, "An improved digital current control of a PM synchronous motor with a simple feedforward disturbance compensation scheme" Proceedings of the IEEE International Conference on PESC'98, pp. 101-107, 1998.

[12] K. Youcef-Toumi and O. Ito, "A time delay controller for systems with unknown dynamics" ASME Journal of Dynamic Systems, Measurement, and Control, Vol. 112, pp. 133-142, 1990, March

[13] T. C. Hsia and L. S. Gao, "Robot manipulator control using decentralized linear time-invariant time-delayed joint controllers" Proceedings of the IEEE International Conference on Robotics and Automation, pp. 2070-2075, 1990.

[14] K.Ogata, Discrete time Control Systems, Prentice-Hall, 1987.

[15] H.W.van der Broeck, H.C.Skudelny, and G.V. Stanke, "Analysis and realization of a pulsewidth modulator based on voltage space vectors" IEEE Trans. Ind. Appl., Vol. 24, No. 1, pp. 142-150, 1988, Jan./Feb.

[16] TMS320C3x User's Guide, Texas Instrument, 1990.

< 저 자 소 개 >

김경화(金庚和)

1969년 3월생. 1991년 2월 한양대 공대 전기공학과 졸업(학사). 1993년 2월 한국과학기술원 전기 및 전자공학과 졸업(석사). 1998년 2월 동 대학원 전기 및 전자공학과 졸업(박사). 1998년-현재 삼성전자 냉공조사업부 선임연구원.

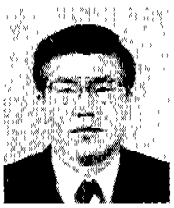

윤명중(尹明重)

1946년 11월생. 1970년 서울대 졸업. 1974년 University of Missouri-Columbia 졸업(석사). 1978년 동 대학원 졸업(박사). 1978년부터 General Electric Columbia에서 Individual Contnbutor on Aerospace Electrical Engineering으로 재직. 현재 한국과학기술원 전기 및 전자공학과 교수. 당 학회 회장 역임.